STUDIA UNIVERSITATIS BABEŞ-BOLYAI, CHEMIA, XLVIII, 1, 2003

HEX TUBES FROM SQUARE TUBES

MIRCEA V. DIUDEA[a*], OLEG URSU[b] and BAZIL PARV[c]

[a] *Faculty of Chemistry and Chemical Engineering, Babes-Bolyai University, 3400 Cluj, Romania*
[b] *Department of Chemistry, Cleveland State University 2121 Euclid Avenue, Cleveland, OHIO 44115 USA*
[c] *Department of Computer Science, Faculty of Mathematics, Babes-Bolyai University, 3400 Cluj, Romania*

ABSTRACT. Single wall nanotubes, covered by hexes can be generated from square tiled lattices, embedded on the cylinder. This route enables the "in silico" synthesis of a variety of tubes: crenelated (*i.e*., armchair, or acenic), zig-zag (or phenacennic), as well as twisted (*i.e*., chiral) objects. The energetic stability and topological characterization of such pure carbon lattices is discussed.

INTRODUCTION

Novel forms of carbon allotropes, besides ancient graphite and diamond, have been designed and obtained by condensing the vaporised graphite.[1] Finite molecular cages have been synthesised, characterised, functionalized or inserted into some supramolecular compounds.[2-6] Besides the well known near-spherical fullerenes, cylinders, capped tubules and tori have aroused both theoretical and experimental interest.[7-23] Multi elemental large cages have also been studied.[24]

This paper describes a novel way of generating single-walled nanotubes SWNTs, starting from square tiled cylinders. Several cutting procedures and transformations of the square nets are proposed in the view of obtaining chemically significant lattices. The stability of SWNTs, as given by the MM+ energy calculations, is discussed.

SQUARE AND HEX NET GENERATION

Covering a cylindrical surface by hexagons (and other polygons) is mainly achieved by the graphite zone-folding procedure, as follows.[25,26]

A SWNT is generated by rolling up a graphite sheet (despite the metal nanoparticle catalyzed tube synthesis suggests a different way). The structural characteristics (diameter and helicity) are uniquely characterized by the roll-up vector $Ch = na + mb$ with a and b being the graphite net vectors and n, m

integers. The translation vector *T* follows the tube axis and is orthogonal to *Ch*. The rolled up area, delimited by *T* and *Ch* (Figure 1) corresponds to the repeat unit of an (*n*,*m*) chiral tube, (3,2) in this example. The limiting, achiral cases, (*n*,0) zigzag or phenacenic, and (*n*,*n*) armchair or acenic, are drown with dashed lines in Figure 1.

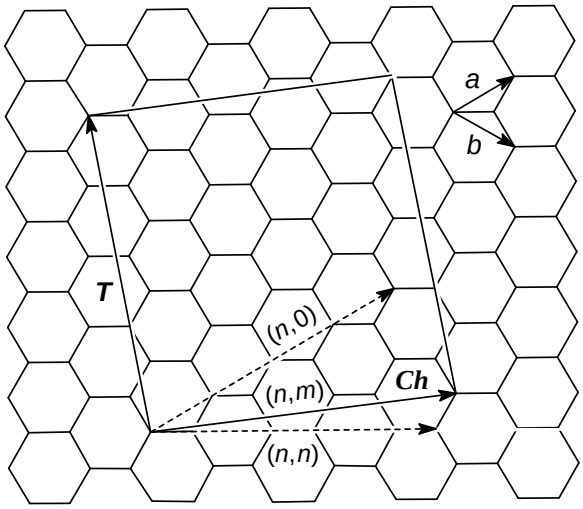

Figure 1. A graphite sheet with its net vectors *a* and *b* and the roll-up vector *Ch* = *na* + *mb* and the translation vector *T*, along the tube axis and normal to *Ch*. The chiral (*n*,*m*) tube is actually a (3,2) tube. The achiral cases: (*n*,0) zigzag and (*n*,*n*) armchair are indicated by dashed lines.

In our procedure, a cylindrical surface is covered by squares by moving a cross section *c*-fold polygon along the cylinder generator Figure 2,a). Next, bonds are alternatively removed in order to change the squares into hexagons. If the deleted edges laid *horizontally* (*i.e*., parallel to the cylinder generator) a standard HC_6 (*i.e*., a phenacenic) pattern results (Figure 2,b). If v*ertical* edges are cut off, a standard VC_6 (*i.e*., an acenic) pattern is obtained (Figure 2,c). Several cutting procedures have been developed in this respect.[19-23]

TUC_4 [6,8] (a) $TUHC_6$ [6,8] (b)

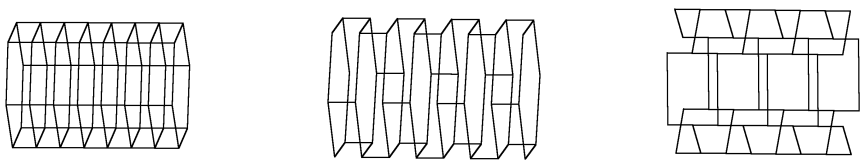

Figure 2. A square cylindrical net (a) and its derived HC_6 (b) and VC_6 (c) patterns.

After optimising by a molecular mechanics program, the polyhex nanotubes look like in Figure 3. The phenacenic (*i.e*., HC_6 patterned) tube ends in "zig-zag" while the tips of the acenic (*i.e*., VC_6 patterned) one are "crenelated" (or "armchair").

$TUHC_6[12,n]$ (a) $TUVC_6[12,n]$ (b)

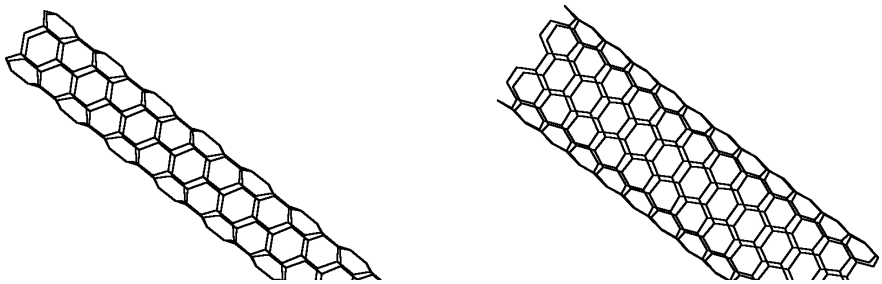

Figure 3. A phenacenic (*i.e*., zigzag – (a)) and an acenic (*i.e*., armchair) tube.

Note that, by cutting some edges within a torus, a spanning tube can be obtained. The name of a tube, *e.g*., $TUHC_6[12,n]$, is derived from that of the original torus. The two first letters come from "tube", the third one specifies the type of cut edges, further letters and numbers denote the type of tiling. In brackets, the (combinatorial) dimensions of the net are given: *c*-fold cross-section polygon and *n*-slices of the cylinder. Tne number of points (*i.e*., atoms) in the structure is $N = c \cdot n$.

Let's now switch the connections, in a horizontal row of squares, one edge to the right (or to the left – Figure 4, a). Next, cut horizontal (Figure 4, b) or vertical (Figure 4, c) edges in an alternating manner (see above). Twisted nets are thus obtained. Note that the number of switched rows must be even for a pure polyhex net.

$TU2C_4$ [6,8] (a) $TUH2C_6$ [6,8] (b) $TUV2C_6$ [6,8] (c)

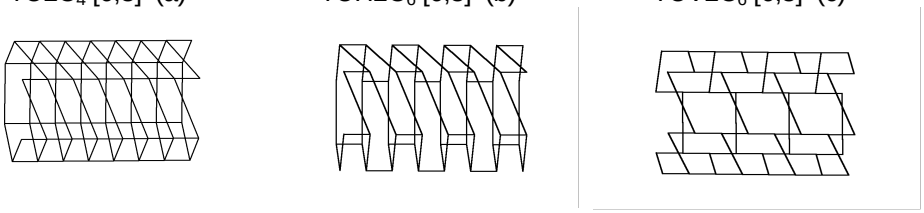

Figure 4. Cylindrical twisted nets, covered by: squares (a), H-hexes (b) and V-hexes (c)

After optimization, the polyhex tubular net is a chiral one (see below). The name of the twisted tubes is formed by adding, after the letter of cut type, the number of twisted rows *t*, *e.g*., $TUVtC_6$ [*c*,*n*].

A CHIRAL TUBE FAMILY: TU*t*C_6 [12,60].

In the following, a family of twisted nanotubes is presented. First, their topology is given: number of hexes *h*, number of zig-zag's *zz*, and number of crenels *cr*. Also given are the length *L* and tube diameter *d* (in Angstroms - see Figures 5 and Table 1).

TUVC_6 [12,60]
L = 71.54; d = 8.04; h =12; zz = 0; cr = 6

TUV2C_6 [12,60]
L =70.53; d = 8.04; h =12; zz = 2; cr = 5

TUHC_6 [12,60]
L = 124.07; d = 4.71; h = 6; zz = 6

TUH2C_6 [12,60]
L = 120.93; d = 4.75; h = 7; zz = 7

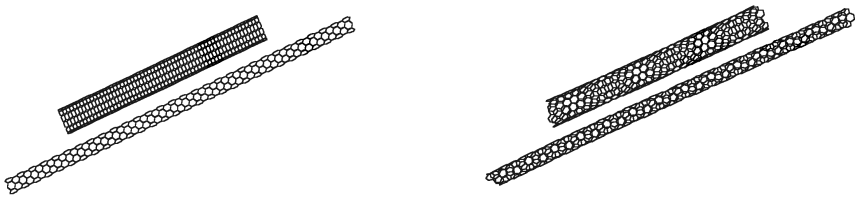

Figure 5. a.

TUV4C_6[12,60]
L =69.04; d =8.18; h =12; zz = 4; cr = 4

TUV6C_6[12,60]
L =67.97; d = 8.23; h = 12; zz = 6; cr = 3

TUH4C_6[12,60]
L =110.20; d =5.39; h = 8; zz = 8

TUH6C_6[12,60]
L =95.76; d =6.14; h = 9; zz = 9

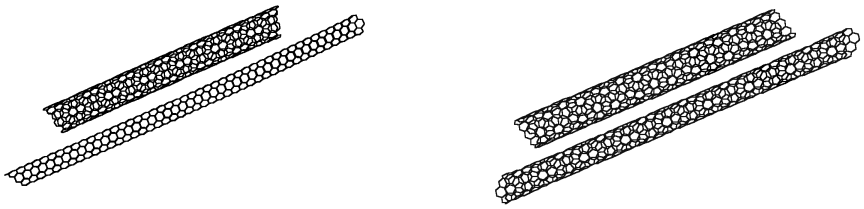

Figure 5. b.

TUV8C_6[12,60]
L = 66.57; d = 8.57; h =12; zz = 8; cr = 2

TUV10C_6[12,60]
L = 63.68; d =8.88; h = 12; zz = 10; cr = 1

TUH8C_6[12,60]
L = 81.92; d = 7.09; h =10; zz = 10

TUH10C_6[12,60]
L = 70.25; d = 8.13; h = 11; zz = 11

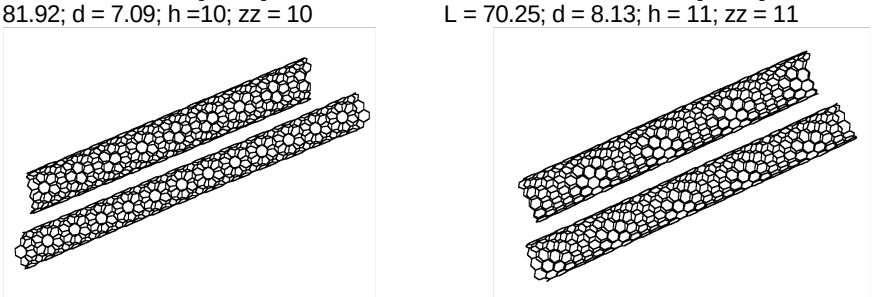

Figure 5. c.

TUV12C_6[12,60]
L = 61.65; d = 9.26; h =12; zz = 12; cr = 0

TUH12C_6[12,60]
L = 61.65; d = 9.26; h =12; zz = 12

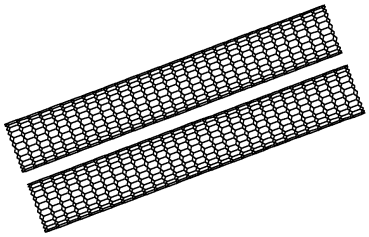

TUHC_6[24,30]
L = 61.65; d = 9.26; h =12; zz = 12

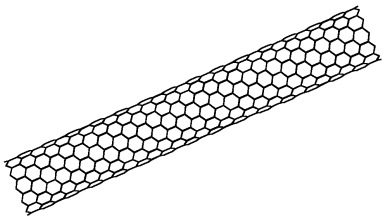

Figure 5. d.

At $t = c$, TUHtC$_6$ [c,n] switches the class of size (*i.e.*, becomes twice thick and half long), while TUVtC$_6$ [c,n] switches the class of cutting (becoming a H-cut tube).

Encoding the type of tessellation can be achieved by means of the ring spiral code.[27,28] It was first proposed for coding and constructing spherical fullerenes. Diudea[29] proposed recently a modification, useful in tubular structures. In a periodic tubular net, the spiral code brings information on size and sequence of faces and embedding the actual net on the parent all-C$_4$ [c,n]. The spiral code for the polyhex tubes is given in Table 1. Also included in this table are the net parameters (for calculating, by the spiral code formulas, the number of hexes in the cross-section of twisted tubes - in general non-integer numbers, as exemplified in Table 2) as well as the number of zig-zags and crenels, as twisting feature data.

Table 1.

Formulas for the spiral code, net parameters and the number of zig-zags (crenels).

Tube	Spiral code	Net parameters	*zz*; {*cr*}
TUHC$_6$[c,n]	$[6_{c/2}]_{(n-1)}$	c; n	$c/2$
TUHtC$_6$[c,n]	$[\,(6_{c/2})_t\,]_{(n-1)/t}$	$c' = c/(1-t/2c)$ $n' = n(1-t/2c)$	$(c+t)/2$
TUVtC$_6$ [c,n]	$[(6_c)_t]_{\{[n-(2+z)]+cz\}/2t}$	c; n $2c$; $n/2$	t; $\{(c-t)/2\}$
TUVC$_6$[c,n]	$[6_c]_{\{[n-(2+z)]+cz\}/2}$	c; n	$\{c/2\}$

$z = \mathrm{mod}(n,2)$

Table 2

Parameters of the TUH(V)tC$_6$[12,60] family

No	t [12,60]	c'	n'	*Cut type*	*zz*	*k*
	TUH t					
1	0	12	60	H	6	0
2	2	13.091	55	H	7	0
3	4	14.400	50	H	8	0

No	*t* [12,60]	*c'*	*n'*	*Cut type*	*zz*	*k*
4	6	16.000	45	H	9	0
5	8	18.000	40	H	10	0
6	10	20.571	35	H	11	0
7	12	24	30	H	12	0
	TUV *t*					
8	0	12	60	V	0	6
9	2	12	60	V	2	5
10	4	12	60	V	4	4
11	6	12	60	V	6	3
12	8	12	60	V	8	2
13	10	12	60	V	10	1
14	12	24	30	H	12	0

MOLECULAR MECHANICS CALCULATIONS

Our TORUS software package enables generation of huge tubes, up to 20,000 atoms, which could be optimised by a molecular mechanics procedure (see Figures 5).

The energy calculated by MM+ force field (by HyperChem software package)[30] decreases as twisting *t* increases (Table 3). Thiss energy (per atom) is ploted against *t*, with a rather good correlation (Figure 6).

Table 3

MM+ Energy E (Kcal·mol^{-1}) and Wiener index W in tubes TUH(V)*t*C_6[12,60]

t	MM+ E TUH*t*C_6	W	MM+ E TUV*t*C_6	W
0	3697.395	10416420	604.008	6009408
2	3384.387	9277724	585.336	5995628
4	2656.301	8314604	535.643	5953396
6	1814.103	7468448	458.833	5883634
8	1093.638	6724178	361.800	5789712
10	546.411	6083308	253.726	5677120
12	141.162	5553216	141.165	5553216

Compared with the MM+ energy of C_{60} (about 4.454 kcal/mol – per atom value), it appears that the structure of twisted tubes (of the discussed family) quickly stabilise, as *t* increases, a fact confirmed by experimental data.[25]

Note that both series TUH*t*C_6 and TUV*t*C_6 converge to one and the same structure: TUHC_6[24,30], which is a non-chiral nanotube, identical with the totally twisted tubes TUH12C_6[12,60] and TUH(V)12C_6[12,60] (see Tables 2 and 3). This identity holds (at least) for tubes having $n = pc$; p = 1, 2, … The MM+ energy can be predicted, with good accuracy, from the topological distance count, also known as the Wiener index[31,32] (see Table 3 and Figures 7 and 8).

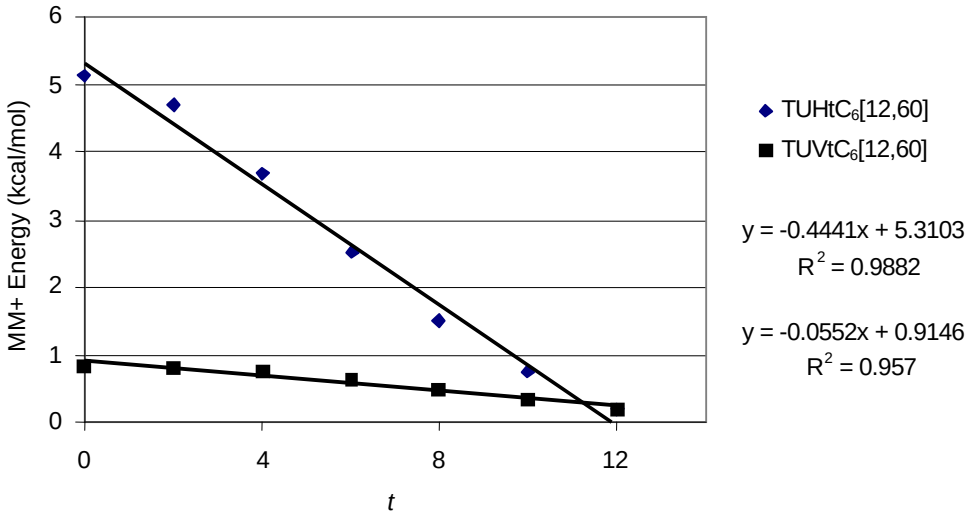

Figure 6. MM^+ energy per atom *vs* twisting *t* in polyhex tubes

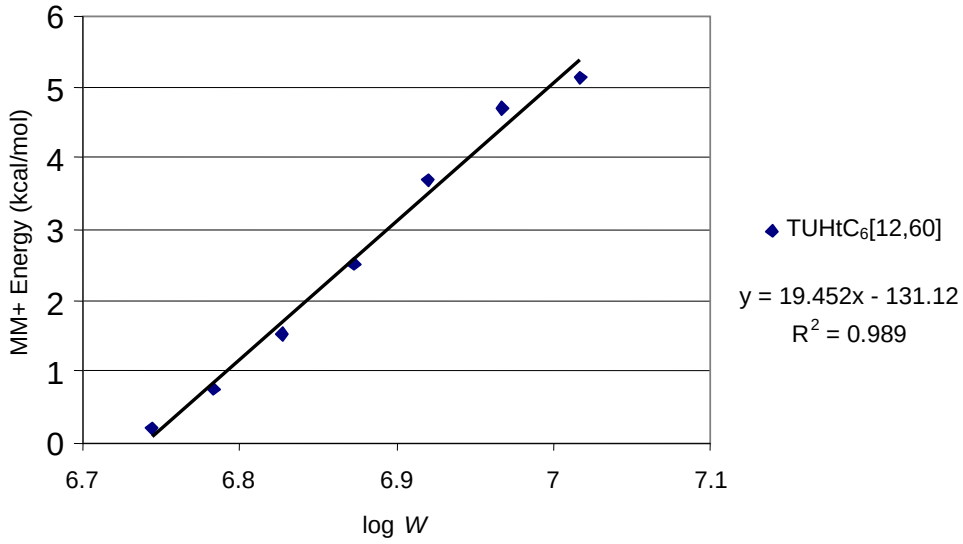

Figure 7. MM^+ energy per atom *vs* log *W* in TUH*t*C_6[12,60] series

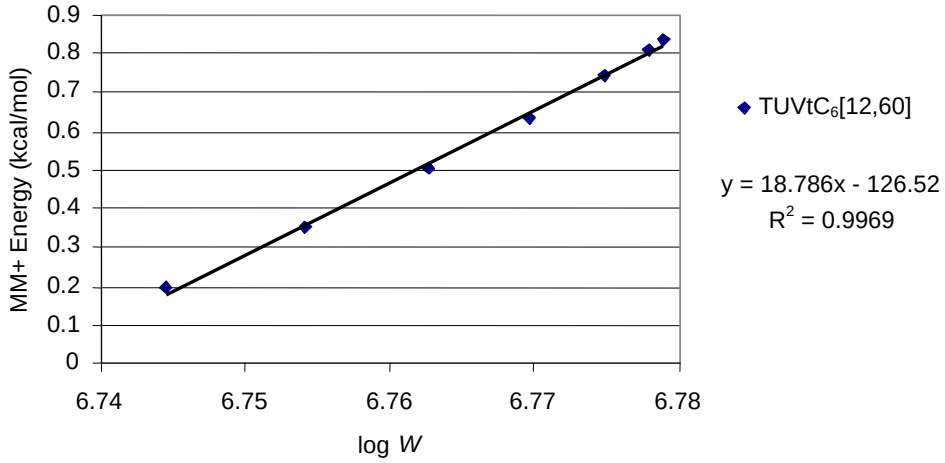

Figure 8. MM^+ energy per atom *vs* log *W* in TUV*t*C_6[12,60] series

CONCLUSIONS

Generation of hex tubes from square tubes, proved to be a simple and versatile method. Topology and enrgetic stability of a family of chiral/twisted nanotubes was invstigated.

By twisting, major changes in the tube topology occur: the tube becomes chiral and, at $t = c$, TUH*t*C_6 [*c*,*n*] switches the class of size, while TUV*t*C_6 [*c*,*n*] switches the class of cutting (becoming a H-cut tube).

Twisting inducees a relaxation of the total MM+ energy of the polyhex tubular net.

MM+ energy can be predicted by a topological descriptor, such as the Wiener index, counting all the topological distances in a given graph. Analytical formulas for calculating this parameter were given elsewhere.[33,34]

Acknowledgement. This paper was supported by the Romanian CNCSIS GRANT 2003.

REFERENCES

1. H. Kroto, *Fuller. Sci. Technol*., **1994**, *2*, 333-342.
2. H. Kroto, J. R. Heath, S. C. O'Brian, R. F. Curl, and R. E. Smalley, *Nature* (London), **1985**, *318*, 162-163.

3. W. Kraetschmer, L. D. Lamb, K. Fostiropoulos and D. R. Huffman, *Nature* (London), 1990, *347*, 354-358.
4. W. Qian and Y. Rubin, *Angew. Chem. Int. Ed*., **2000**, *39*, 3133-3137.
5. K. Lee, Ch. H. Lee, H. Song, J. T. Park, H. Y. Chang and M.-G. Choi, *Angew. Chem. Int. Ed*., **2000**, *39*, 1801-1804.
6. T. F. Fässler, R. Hoffmann, S. Hoffmann and M. Wörle, *Angew. Chem. Int. Ed*., **2000**, *39*, 2091-2094.
7. J. Liu, H. Dai, J. H. Hafner, D. T. Colbert, R. E. Smalley, S. J. Tans and C. Dekker, *Nature*, **1997**, *385*, 780-781.
8. M. Ahlskog, E. Seynaeve, R. J. M. Vullers, C. Van Haesendonck, A. Fonseca, K. Hernadi and J.B. Nagy, *Chem. Phys. Lett*., **1999**, *300*, 202-206.
9. R. Martel, H. R. Shea and Ph. Avouris, *Nature*, **1999,** *398*, 299-299.
10. R. Martel, H. R. Shea and Ph. Avouris, *J. Phys. Chem*., *B,* **1999***, 103,* 7551-7556.
11. D. Babić, D. J. Klein and T. G. Schmalz, *J. Mol. Graphics Modell.*, **2001**, *19*, 222-231.
12. A. Ceulemans, L. F. Chibotaru and P. W. Fowler, *Phys. Rev. Lett*., **1998**, *80*, 1861-1864.
13. J. K. Johnson, B. N. Davidson, M. R. Pederson and J. Q. Broughton, *Phys. Rev*., *B*, **1994**, *50*, 17575-17582.
14. E. C. Kirby, *Croat. Chem. Acta*, **1993**, *66*, 13-26
15. E. C. Kirby, R. B. Mallion and P. Pollak, *J. Chem. Soc. Faraday Trans*., **1993**, *89*, 1945-1953.
16. A. Ceulemans, L. F. Chibotaru, S. A. Bovin and P. W. Fowler, *J. Chem. Phys*., **2000**, *112*, 4271-4278.
17. D. Marušić and T. Pisanski, *Croat. Chem. Acta*, **2000**, *73*, 969-981.
18. E. C. Kirby and P. Pollak, *J. Chem. Inf. Comput. Sci*., 1998, *38*, 66-70.
19. M. V. Diudea and A. Graovac, *Commun. Math. Comput. Chem*. (*MATCH*), 2001, *44*, 93-102.
20. M. V. Diudea, I. Silaghi-Dumitrescu and B. Parv, *Commun. Math. Comput. Chem*. (*MATCH*), **2001**, *44*, 117-133.
21. M. V. Diudea and E. C. Kirby, *Fullerene Sci. Technol.*, **2001**, *9*, 445-465.
22. M. V. Diudea, *Bull. Chem. Soc. Japan*, **2002**, *75*, 487-492.
23. M. V. Diudea, *Fullerenes, Nanotubes,Carbon Nanostruct.*, **2002**, *10*, 273-292.
24. A. Müller, P. Kögerler and Ch. Kuhlmann, *Chem. Commun*., **1999**, 1347-1358.
25. T. W. Odom, J.-L. Huang, Ph. Kim and Ch. M. Lieber,*J. Phys. Chem. B*., **2000**, *104*, 2794-2809.
26. A. L. Ivanovskii, *Russ. Chem. Rev*., **1999**, *68*, 103-118.
27. D. E. Manolopoulos, J. C. May and S. E. Down, *Chem. Phys. Lett*., **1991**, *181*, 105-111.
28. G. Brinkmann, P. W. Fowler and M. Yoshida, *Commun. Math. Comput. Chem*. (*MATCH*), **1998**, *38*, 7-17.
29. M. V. Diudea, *Phys. Chem., Chem. Phys.*, **2002**, *4*, 4740-4746.

30. HyperChem [TM], release 4.5 for SGI, © 1991-1995, HyperCube, Inc.
31. H. Wiener, *J. Am. Chem. Soc.,* **1947***, 69*, 17-20.
32. M.V. Diudea; I. Gutman; L. Jäntschi, *Molecular Topology*, Nova Science, Huntington, New York, 2001.
33. P. E. John and M. V. Diudea, *Croat. Chem.Acta,* **2003** (submitted).
34. M. V. Diudea, M. Stefu, B. Parv and P. E. John, *Croat. Chem. Acta,* **2003** (submitted).